SCIENTIFIC CULTURE
www.sci-cult.com

SCIENTIFIC CULTURE, Vol. 12, No. 1.1, (2026), pp. 4707-4714
Open Access. Online & Print

DOI: 10.5281/zenodo. 121126327

CORRELATION OF MECHANICAL PROPERTIES WITH ADDITIVE MANUFACTURING (FDM) IN TYPE I PLA SPECIMENS BASED ON ASTM D638-22

Alberto Delgado Hernandez[1], Benjamín González Vizcarra[2*], Ana María Castañeda[3], Miguel Ángel Ávila Puc[4], Miriam Siqueiros Hernández[5]

[1,2,4]Universidad Autónoma de Baja California, Facultad de Ciencias de la Ingeniería y Tecnología, México.
[3] Universidad Autónoma de Baja California, Facultad de Ingeniería Mexicali, México.
[4] Universidad Autónoma de Baja California, Facultad de Ingeniería Mexicali, México.

Received: 01/12/2025
Accepted: 02/01/2026

Corresponding author: Islam Elgammal
(I.elgammal@ubt.edu.sa)

ABSTRACT

This study analyzes the tensile mechanical properties of polylactic acid (PLA) manufactured using fused deposition modeling (FDM), a widely used technique in the fabrication of polymeric parts due to its accessibility and dimensional stability (Raj et al., 2018; Travieso-Rodríguez et al., 2019). The analysis was conducted according to the ASTM D638-22 standard, using Type I specimens, a methodology commonly applied in the tensile characterization of PLA-printed materials (Agaliotis et al., 2022; Atakok et al., 2022). Three infill density levels (50%, 75%, and 100%) were evaluated to determine their influence on the strength, elastic modulus, and elongation of the material, considering that infill density is a critical parameter that directly affects the stiffness and load-bearing capacity of printed PLA (Karad et al., 2023; Raja et al., 2022). The specimens were printed with horizontal orientation and controlled parameters for temperature, speed, and infill pattern, under standardized environmental conditions, as recommended in prior studies to ensure reproducibility of mechanical results (Ali et al., 2023; Kumar et al., 2023). The results show a direct correlation between infill density and material stiffness: the 100% infill specimens achieved the highest values of maximum stress (38.3 MPa) and elastic modulus (1061 MPa), while the 50% infill specimens exhibited greater deformability. This trend aligns with studies reporting significant strength increases as infill percentage rises (Khalili et al., 2023; Stoia & Linul, 2024). The study confirms that infill density is a key parameter for optimizing the mechanical properties of 3D-printed PLA, providing valuable insights for the design of functional components in additive manufacturing (Alex et al., 2025; Son Minh et al., 2024).

KEYWORDS: PLA, 3D printing, tensile testing, ASTM D638, infill density, elastic modulus.

1. INTRODUCTION

Additive manufacturing, commonly known as 3D printing, has revolutionized the way products are designed and fabricated, enabling the creation of complex and customized geometries without the need for molds or specific tooling. Among the available technologies, fused deposition modeling (FDM) has become one of the most widely used due to its low cost, versatility, and ease of use in academic, research, and production environments.

Polylactic acid (PLA) is one of the most frequently employed polymers in FDM 3D printing, owing to its renewable origin, biodegradability, low toxicity, and acceptable mechanical strength. These characteristics make it a sustainable alternative to petroleum-derived materials. However, its mechanical properties are highly dependent on printing parameters such as extrusion temperature, layer orientation, deposition speed, and notably, infill density and pattern.

In engineering applications, controlling the infill density of 3D-printed PLA parts allows for adjusting structural stiffness and strength without modifying the external geometry. A higher infill percentage increases the component's strength and rigidity, while a lower percentage reduces weight, material consumption, and printing time. This flexibility makes PLA an ideal material for the design of lightweight functional parts, structural prototypes, and components with specific mechanical requirements.

Optimizing the infill not only enhances mechanical performance but also represents an opportunity to advance toward more sustainable manufacturing processes. Reducing material usage and printing time leads to lower energy consumption and less waste generation, aligning with the principles of green engineering and responsible production. In this context, systematically analyzing the effect of infill density on the tensile properties of PLA enables the identification of configurations that balance structural efficiency, resource savings, and functional performance.

The objective of this study is to evaluate the tensile mechanical behavior of 3D-printed PLA at different infill density levels (50%, 75%, and 100%), using Type I specimens in accordance with the ASTM D638-22 standard. The experimental results allow for establishing the relationship between infill density and the fundamental mechanical properties of the material, aiming to optimize the design of functional parts that combine high strength, low weight, and environmental sustainability.

2. MATERIALS AND METHODS

The material used was ENDER® brand PLA filament, white color, 1.75 mm in diameter, considering that PLA is one of the most commonly used polymers in FDM processes due to its commercial availability and mechanical stability (Caminero et al., 2019; Plamadiala et al., 2025). The specimens were fabricated using a Creality CR-10S5 printer with FDM technology and a 0.4 mm nozzle, a standard configuration in experimental studies aimed at evaluating the mechanical properties of PLA (Nugroho et al., 2018; Gao et al., 2022).

Three infill densities were defined (50%, 75%, and 100%), using a Rectilinear/Grid pattern (0/90°), three perimeters, five top and bottom layers, and a 12% infill-to-wall overlap. These parameters have been identified as crucial factors influencing the stiffness and strength of printed materials (Karad et al., 2023; Raja et al., 2022). Printing was performed in a horizontal orientation with a layer height of 0.20 mm, a speed of 50 mm/s, a hotend temperature of 225 °C, and a heated bed at 65 °C, consistent with previous recommendations to ensure adequate interlayer adhesion (Kumar et al., 2023; Ali et al., 2023). Each set of conditions was replicated eight times to ensure statistical repeatability of the results, a practice supported by similar experimental evaluations (Atakok et al., 2022; Agaliotis et al., 2022). The specimens were visually inspected to eliminate printing defects prior to testing, a common control measure to ensure the validity of mechanical tests.

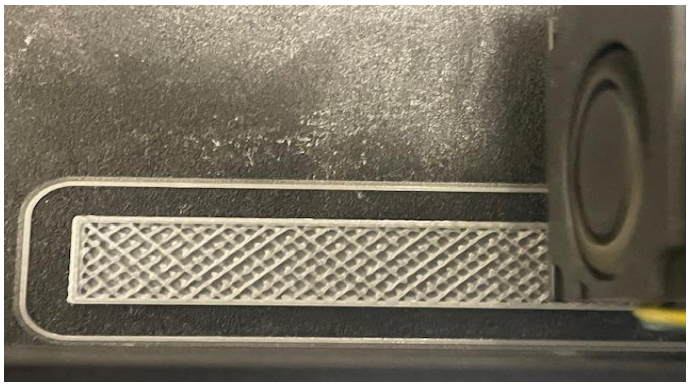

Figure 1: Printing process of PLA specimens using FDM technology with Grid infill pattern.

As shown in Figure 1, the specimens were printed using a diagonal mesh infill pattern, ensuring a uniform material distribution and adequate interlayer adhesion—an aspect highlighted in studies on the mechanical performance of printed PLA (Kumar et al., 2023).

Tensile tests were conducted according to the ASTM D638-22 standard using Type I specimens with dimensions of 165 mm total length, 57 mm gauge length, 13 mm width at the narrow section, and a nominal thickness of 3.2 mm. The use of Type I specimens under ASTM D638 is a widely adopted standard for the mechanical characterization of printed polymeric materials (Agaliotis et al., 2022; Atakok et al., 2022). A 50 mm gage length extensometer was used with a crosshead speed adjusted for failure within 0.5–5 minutes, ensuring a strain rate in accordance with the standard. Tests were conducted on a Shimadzu® AGS-X universal testing machine with a 100 kN load capacity under conditions of 23 ± 2 °C and 50 ± 5% relative humidity, using Trapezium X® software.

Figure 2: Tensile test setup for a Type I specimen according to ASTM D638-22 using a Shimadzu® AGS-X machine

As shown in Figure 2, the specimen was clamped in the grips of the universal testing machine, ensuring proper axial alignment and preventing slippage during load application. This setup enabled the acquisition of precise and repeatable stress–strain curves, consistent with the brittle behavior typically reported for PLA in previous literature (Stoia & Linul, 2024; Seol et al., 2018).

The stress–strain curves obtained for each specimen were analyzed using Microsoft Excel®, identifying the initial elastic region, yield point, maximum stress, and stress at break. The slope of the elastic region was used to determine Young's modulus, while the plastic regions were analyzed through linear regression to obtain representative equations and determination coefficients (R^2) for each specimen. The application of linear regressions to model the mechanical behavior of PLA has shown reliable results in recent studies, with determination coefficients exceeding 0.90 (Son Minh et al., 2024; Mencarelli et al., 2025).

3. RESULTS AND DISCUSSION

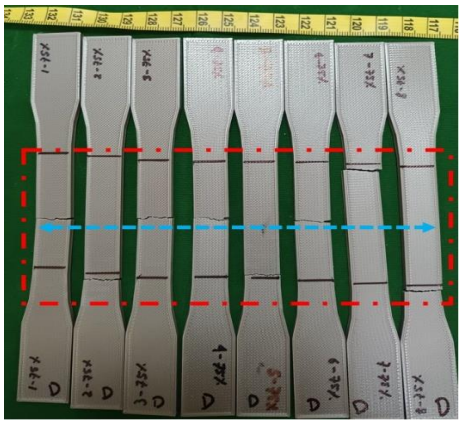

Figure 3: PLA specimens after tensile testing showing typical fracture location.

As shown in Figure 3, the fractures consistently occurred in the calibrated section of the specimens, which confirms correct alignment and proper testing conditions. The fracture surfaces were clean and perpendicular to the loading axis, with slight indications of brittle failure, in agreement with the characteristic response of PLA reported in previous literature (Travieso-Rodríguez et al., 2019; Raj et al., 2018).

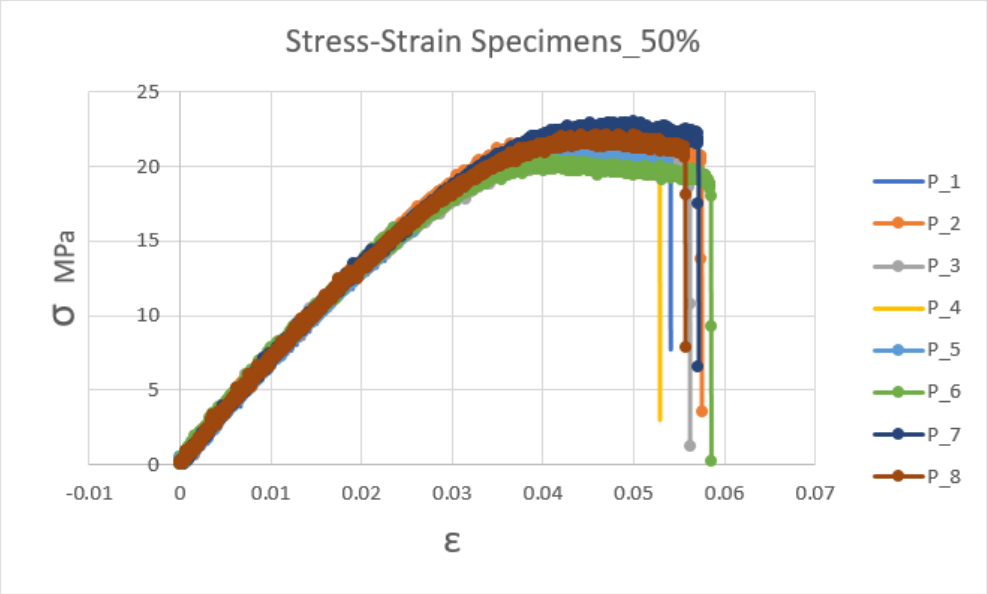

Figure 4: Stress–strain curves for the eight PLA specimens with 50% infill.

Figure 4 shows the stress–strain curves for the eight PLA specimens with 50% infill. These curves exhibit greater variability among specimens, with lower initial slopes and more ductile behavior compared to higher infill levels. This phenomenon has been reported in studies where reduced infill percentages lead to lower structural stiffness (Karad et al., 2023; Raja et al., 2022).

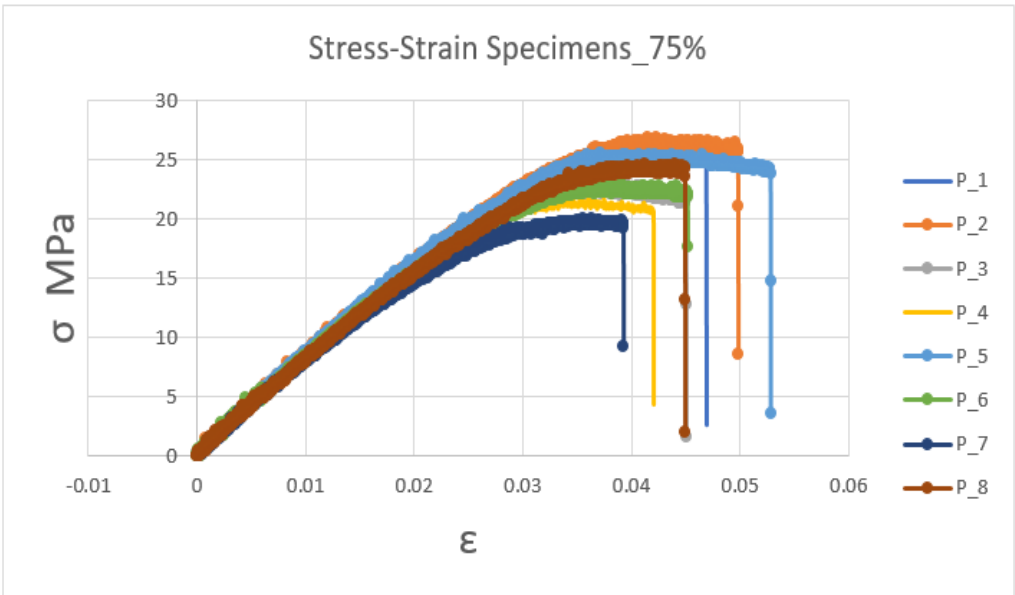

Figure 5: Stress–strain curves for the eight PLA specimens with 75% infill.

Figure 5 displays the stress–strain curves for the eight PLA specimens with 75% infill. In this group, a more consistent mechanical response is observed, with steeper initial slopes and a maximum stress that falls between the values obtained for 50% and 100% infill. This trend aligns with research findings that indicate gradual increases in strength with intermediate infill levels (Ali et al., 2023; Atakok et al., 2022).

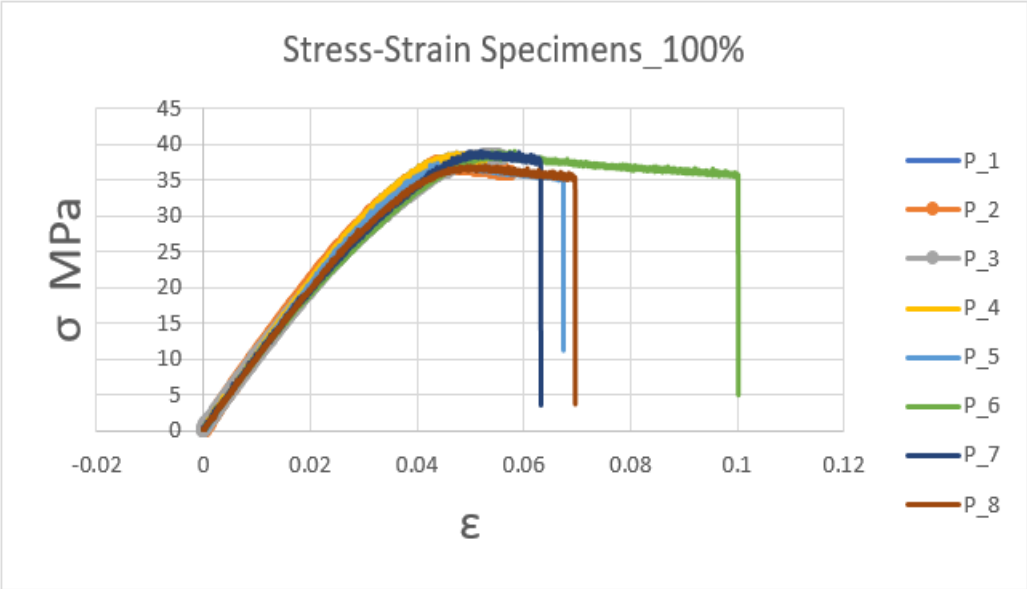

Figure 6: Stress–strain curves for the eight PLA specimens with 100% infill.

Figure 6 presents the stress–strain curves for the eight PLA specimens with 100% infill. These curves exhibit the highest stiffness, steepest slopes, and greatest maximum stress, clearly demonstrating the direct influence of infill on mechanical performance. This observation is consistent with studies reporting significant improvements in strength for infill densities near 100% (Khalili et al., 2023; Son Minh et al., 2024).

The stress–strain curves obtained for the PLA specimens reveal a typically brittle behavior, with a well-defined initial elastic region followed by moderate strain hardening prior to fracture. This behavior is consistent with that reported for PLA manufactured via FDM (Stoia & Linul, 2024; Seol et al., 2018). Figure 3 shows the fractured specimens after tensile testing, highlighting that the failures predominantly occurred in the central zone as specified in the ASTM D638-22 standard.

Table 1: Average tensile mechanical properties of 3D-printed PLA for different infill densities (ASTM D638-22, n = 8 per group).

Infill Density (%)	Young's E Modulus (MPa)	Deformation Yield Limit (mm)	Yield Limit Stress (Mpa)	Maximum stress σmax (MPa)	Deformation at maximum stress (mm)	Stress at Rupture σrupt (MPa)	Deformation at rupture εrupt (mm)
50	705 ± 34	0.0232	14.86	21.6 ± 0.9	0.0445	15.1 ± 3.9	0.0557
75	866 ± 28	0.0205	15.97	23.8 ± 2.3	0.0381	16.2 ± 3.0	0.0458
100	1061 ± 71	0.0260	25.25	38.3 ± 0.8	0.0501	33.2 ± 3.0	0.071

As summarized in Table 1, the results show that stiffness (E) and maximum stress (σ_max) increase significantly with infill percentage. The Young's modulus for 100% infill is approximately 50% higher than that of 50% infill, and the maximum stress increases by nearly 77%—values comparable to those observed in recent studies on PLA printed with higher infill densities (Alex et al., 2025; Mencarelli et al., 2025). The fracture behavior indicates that 100% infill specimens can sustain higher levels of deformation before failure, a trend also reported in reinforced materials or those with greater internal material continuity (Khalili et al., 2023).

As shown in Table 2, the regression analysis of the stress–strain curves confirmed these trends. In the elastic region, the average slope of the curves increased from 704.6 to 1060.8 when going from 50% to 100% infill, with average determination coefficients (R^2) between 0.90 and 0.94. In the plastic region, the average slopes also increased with infill density (from 305.5 to 556.3), with R^2 values above 0.93. These results highlight that increasing material content contributes to greater initial stiffness as well as a more stable response in the post-yield region, in alignment with statistical models previously applied in the mechanical analysis of printed PLA (Son Minh et al., 2024; Mencarelli et al., 2025).

Table 2: Statistical summary of slopes and determination coefficients (R^2) obtained by linear regression in the elastic and plastic zones.

Group	Zone	Average slope (m)	Standard deviation	Average R^2
P_50	Elástica	704.6	34.1	0.90
P_75	Elástica	866.2	27.5	0.93
P_100	Elástica	1060.8	70.7	0.94
P_50	Plástica	305.5	21.0	0.93
P_75	Plástica	431.8	26.4	0.96
P_100	Plástica	556.3	31.2	0.97

Table 3: Average resilience, plasticity, and toughness energy for each infill density.

Infill Density (%)	Resilience (MJ/m^3)	Plasticity (MJ/m^3)	Tenacity (MJ/m^3)
50	0.1728	0.6133	0.6704
75	0.1635	0.5795	0.5792
100	0.3277	1.2600	2.0283

As shown in Table 3, the energy-based results indicate that the energy absorption capacity of PLA increases significantly with the infill percentage. The material's toughness—defined as the total area under the stress–strain curve—increased from 0.6704 MJ/m^3 at 50% to 2.0283 MJ/m^3 at 100%, representing an increase of nearly 200%. This behavior confirms that specimens with higher density exhibit not only greater stiffness and strength but also a higher tolerance to deformation prior to fracture.

Plastic energy also showed an increasing trend, rising from 0.6133 MJ/m^3 to 1.2600 MJ/m^3, indicating that the post-yield region significantly contributes to energy dissipation in the 100% infill specimens. In contrast, resilience values were relatively similar between 50% and 75%, but showed a notable increase at 100%, suggesting a greater capacity for elastic energy storage before yielding begins.

These findings complement the previous mechanical analyses and provide a more comprehensive characterization of the structural behavior of 3D-printed PLA. The assessment of resilience, plastic, and toughness energy helps describe the polymer's ability to store, dissipate, and absorb energy before failure—an approach commonly applied in energy-based analyses of metallic and polymeric materials (Gonzalez-Vizcarra et al., 2021).

From a practical perspective, parts printed at 100% infill offer the best structural performance under tensile loads. However, parts printed at 50% and 75% may be suitable for applications where reducing material use and printing time takes precedence over achieving maximum strength, as suggested in studies focused on printing efficiency and process optimization (Alex et al., 2025; Fischbach & Weinberg, 2023).

4. CONCLUSIONS

The experimental analysis of PLA specimens printed using FDM and tested according to the ASTM D638-22 standard demonstrated that infill density has a significant effect on the tensile properties of the material, as previously noted in studies on the influence of printing parameters on PLA's mechanical performance (Karad et al., 2023; Ali et al., 2023). Increasing infill from 50% to 100% led to approximately a 50% increase in Young's modulus and over a 70% increase in maximum stress, confirming that internal material continuity is a determining factor in load-bearing capacity—consistent with trends reported in recent research (Raja et al., 2022; Khalili et al., 2023).

Specimens with 100% infill exhibited the highest values of elastic modulus, maximum stress, and stress at break, making them suitable for applications where structural strength is a priority. This behavior aligns with findings indicating that high infill densities significantly enhance the stiffness and strength of printed PLA (Son Minh et al., 2024; Mencarelli et al., 2025). Specimens with 50% and 75% infill showed lower load-bearing capacity but may be considered viable options in contexts where reducing material usage or fabrication time is desired, provided the service demands are moderate. This supports recommendations focused on efficiency and sustainability in additive manufacturing (Alex et al., 2025; Fischbach & Weinberg, 2023).

The use of calibrated stress–strain curves, combined with regression fitting in the elastic and plastic zones, enabled the development of a quantitative model for the behavior of printed PLA, with determination coefficients (R^2) generally exceeding 0.90. This methodological approach reinforces the reliability of the results and can be extended to future studies aimed at evaluating the effects of other printing parameters, such as layer orientation, infill pattern, or extrusion temperature—factors already identified as critical variables in previous investigations (Kumar et al., 2023; Atakok et al., 2022).

REFERENCES

Agaliotis, E. M., Ake-Concha, B. D., May-Pat, A., Morales-Arias, J. P., Bernal, C., Valadez-Gonzalez, A., Herrera-Franco, P. J., Proust, G., Koh-Dzul, J. F., Carrillo, J. G., & Flores-Johnson, E. A. (2022). Tensile behavior of 3D printed polylactic acid (PLA) based composites reinforced with natural fiber. *Polymers, 14*(19). https://doi.org/10.3390/polym14193976

Alex, Y., Divakaran, N. C., Pattanayak, I., Lakshyajit, B., Ajay, P. V., & Mohanty, S. (2025). Comprehensive study of PLA material extrusion 3D printing optimization and its comparison with PLA injection molding through life cycle assessment. *Sustainable Materials and Technologies, 43*. https://doi.org/10.1016/j.susmat.2024.e01222

Ali, S., Abdallah, S., Devjani, D. H., John, J. S., Samad, W. A., & Pervaiz, S. (2023). Effect of build parameters and strain rate on mechanical properties of 3D printed PLA using DIC and desirability function analysis. *Rapid Prototyping Journal, 29*(1), 92–111. https://doi.org/10.1108/RPJ-11-2021-0301

Al-Tamimi, A. A., Pandžić, A., & Kadrić, E. (2023). Investigation and prediction of tensile, flexural, and compressive properties of tough PLA material using definitive screening design. *Polymers, 15*(20). https://doi.org/10.3390/polym15204169

Atakok, G., Kam, M., & Koc, H. B. (2022). Tensile, three-point bending and impact strength of 3D printed parts using PLA and recycled PLA filaments: A statistical investigation. *Journal of Materials Research and Technology, 18*, 1542–1554. https://doi.org/10.1016/j.jmrt.2022.03.013

Caminero, M. Á., Chacón, J. M., García-Plaza, E., Núñez, P. J., Reverte, J. M., & Becar, J. P. (2019). Additive manufacturing of PLA-based composites using fused filament fabrication: Effect of graphene nanoplatelet reinforcement on mechanical properties, dimensional accuracy and texture. *Polymers, 11*(5). https://doi.org/10.3390/polym11050799

El Marouazi, H., van der Schueren, B., Favier, D., Bolley, A., Dagorne, S., Dintzer, T., & Janowska, I. (2021). Great enhancement of mechanical features in PLA based composites containing aligned few layer graphene (FLG), the effect of FLG loading, size, and dispersion on mechanical and thermal properties. *Journal of Applied Polymer Science, 138*(44), 1–23. https://doi.org/10.1002/app.51300

Fischbach, M., & Weinberg, K. (2023). Effect of physical aging on the flexural creep in 3D printed thermoplastic. In *Advanced Structured Materials* (Vol. 194, pp. 115–130). https://doi.org/10.1007/978-3-031-39070-8_7

Gao, G., Xu, F., Xu, J., & Liu, Z. (2022). Study of material color influences on mechanical characteristics of fused deposition modeling parts. *Materials, 15*(19), 1–15. https://doi.org/10.3390/ma15197039

Gonzalez-Vizcarra, B., Figueroa, I. A., Novelo-Peralta, O., Delgado-Hernández, A., Siqueiros-Hernández, M., Castañeda-Guzmán, R., & Díaz, C. G. (2021). Study of the Mechanical-Photoacoustic Properties of Thermally Modified Al-6061-T6. Physics of Metals and Metallography, 122(14), 1634–1639. https://doi.org/10.1134/S0031918X21140088

Kahya, Ç., Tunçel, O., Çavuşoğlu, O., & Tüfekci, K. (2025). Thermal annealing optimization for improved mechanical performance of PLA parts produced via 3D printing. *Polymer Testing, 144*(November 2024). https://doi.org/10.1016/j.polymertesting.2025.108735

Karad, A. S., Sonawwanay, P. D., Naik, M., & Thakur, D. G. (2023). Experimental study of effect of infill density on tensile and flexural strength of 3D printed parts. *Journal of Engineering and Applied Science, 70*(1), 1–17. https://doi.org/10.1186/s44147-023-00273-x

Khalili, A., Kami, A., & Abedini, V. (2023). Tensile and flexural properties of 3D-Printed polylactic acid/continuous carbon fiber composite. *Mechanics of Advanced Composite Structures, 10*(2), 407–418. https://doi.org/10.22075/macs.2023.29500.1466

Kumar, M. S., Farooq, M. U., Ross, N. S., Yang, C. H., Kavimani, V., & Adediran, A. A. (2023). Achieving effective interlayer bonding of PLA parts during the material extrusion process with enhanced mechanical properties. *Scientific Reports, 13*(1), 1–21. https://doi.org/10.1038/s41598-023-33510-7

Lanzotti, A., Grasso, M., Staiano, G., & Martorelli, M. (2015). The impact of process parameters on mechanical properties of parts fabricated in PLA with an open-source 3-D printer. *Rapid Prototyping Journal, 21*(5), 604–617. https://doi.org/10.1108/RPJ-09-2014-0135

Mencarelli, M., Sisella, M., Puggelli, L., Innocenti, B., & Volpe, Y. (2025). Sensitivity Analysis of 3D Printing Parameters on Mechanical Properties of Fused Deposition Modeling-Printed Polylactic Acid Parts. *Applied Mechanics, 6*(1). https://doi.org/10.3390/applmech6010017

Nugroho, A., Ardiansyah, R., Rusita, L., & Larasati, I. L. (2018). Effect of layer thickness on flexural properties

of PLA (PolyLactid Acid) by 3D printing. *Journal of Physics: Conference Series, 1130*(1). https://doi.org/10.1088/1742-6596/1130/1/012017

Plamadiala, I., Croitoru, C., Pop, M. A., & Roata, I. C. (2025). Enhancing Polylactic Acid (PLA) Performance: A Review of Additives in Fused Deposition Modelling (FDM) Filaments. *Polymers, 17*(2), 1–34. https://doi.org/10.3390/polym17020191

Raj, S. A., Muthukumaran, E., & Jayakrishna, K. (2018). A Case Study of 3D Printed PLA and Its Mechanical Properties. *Materials Today: Proceedings, 5*(5), 11219–11226. https://doi.org/10.1016/j.matpr.2018.01.146

Raja, S., Agrawal, A. P., Patil, P. P., Thimothy, P., Capangpangan, R. Y., Singhal, P., & Wotango, M. T. (2022). Optimization of 3D Printing Process Parameters of Polylactic Acid Filament Based on the Mechanical Test. *International Journal of Chemical Engineering, 2022*. https://doi.org/10.1155/2022/5830869

Seol, K.-S., Zhao, P., Shin, B.-C., & Zhang, S.-U. (2018). Infill Print Parameters for Mechanical Properties of 3D Printed PLA Parts. *Journal of the Korean Society of Manufacturing Process Engineers, 17*(4), 9–16. https://doi.org/10.14775/ksmpe.2018.17.4.009

Son Minh, P., Nguyen, V. T., Uyen, T. M. T., Do, T. T., Duong Thi Van, A., & Nguyen Le Dang, H. (2024). The effects of 3D printing designs on PLA polymer flexural and fatigue strength. *Journal of Micromechanics and Microengineering, 34*(6). https://doi.org/10.1088/1361-6439/ad4b2a

Stoia, D. I., & Linul, E. (2024). Tensile, flexural and fracture properties of MEX-printed PLA-based composites. *Theoretical and Applied Fracture Mechanics, 132*(March). https://doi.org/10.1016/j.tafmec.2024.104478

Travieso-Rodriguez, J. A., Jerez-Mesa, R., Llumà, J., Traver-Ramos, O., Gomez-Gras, G., & Rovira, J. J. R. (2019). Mechanical properties of 3D-printing polylactic acid parts subjected to bending stress and fatigue testing. Materials, 12(23). https://doi.org/10.3390/ma12233859